JOURNAL OF APPLIED ELECTROCHEMISTRY **16** (1986) 229–238

The electrochemistry of nitrate–amide melts: reactions of nickel and copper in nitrate–amide melts

G. E. McMANIS, A. N. FLETCHER, D. E. BLISS, M. H. MILES

Energy Chemistry Branch, Chemistry Division, Research Department, Naval Weapons Center, China Lake, California 93555, USA

Received 15 January 1985; revised 17 April 1985

Copper and nickel may be electrodeposited from their ions in solution in nitrate–amide melts at room temperature. In the ammonium nitrate–acetamide–urea melt at 23° C, the reduction to the metal competes with the corrosion reaction at low rates and with the reduction of the ammonium and nitrate ions of the melt at high current densities. Two distinct types of nickel complexes are found in solution. The nickel complex formed by the corrosion reaction is bound by at least one ammonia ligand. Nickel complexes formed by dissolving the halide in the melt show evidence of coordination by less strongly bounding ligands, probably by amides. Similarly, the visible spectra of copper chloride in solution suggest that the cupric ions are coordinated primarily by amides. The copper corrosion reaction produces a complex with a spectra distinctly different from that of cupric chloride in solution. The shift in absorption maxima suggests that the copper complex formed by the corrosion reaction has at least one ammonia ligand in the coordination sphere.

1. Introduction

In two separate communications we detailed some of the characteristics of a novel class of electrolytes, the nitrate–amide melts [1, 2]. The potential utility of nitrate–amide melts as room temperature electrolytes was first reported by Lovering and Gale [3]. Lovering and Clark reported the anodization of several metals including titanium in a NH_4NO_3–urea eutectic melt between 45 and 85° C [4]. Tkalenko and co-workers reported the effects of amides on electrode reactions in molten nitrates at higher temperatures [5–7]. Cherepanov *et al.* studied the effects of urea on the chronopotentiometric reduction of Co^{2+}, Cd^{2+} and Ag^{+} in molten $LiNO_3$–KNO_3 eutectic [8]. Our reports appear to be the first discussion of the chemistry and electrochemistry of nitrate–amide melts at room temperature. We have found that many mixtures of inorganic nitrates and simple amide eutectics (like the acetamide–urea eutectic) form room temperature melts with reasonably high conductivities [1].

Nitrate–amide melts show a remarkable tendency to supercool [1]. A glass transition occurs near −40° C for melts using $LiNO_3$ or NH_4NO_3 electrolytes in an acetamide–urea eutectic solvent. The acetamide–urea eutectic amide melting point is 55° C [9]. A melting point of 7.8° C has been reported for the acetamide–urea–ammonium nitrate eutectic mixture [10]. That eutectic has an ammonium concentration of 0.28 mol fraction and its room temperature (23° C) conductivity is greater than $10^{-3}\,\Omega^{-1}\,cm^{-1}$. Melts using $LiNO_3$ in the acetamide–urea eutectic solvent also form room temperature liquids. However, the $LiNO_3$–amide melts have significantly lower conductivities than those observed for the ammonium nitrate–amide melts [1].

In the ammonium nitrate–amide melts we have found that the predominant cathode reaction is the reduction of ammonium ions to ammonia and hydrogen [1, 2],

$$NH_4^+ + e \longrightarrow NH_3 + \tfrac{1}{2}H_2 \qquad (1)$$

We have reported that the predominant oxidation reaction in the nitrate–amide melts is

$$NO_3^- \longrightarrow NO_2 + \tfrac{1}{2}O_2 + e \qquad (2)$$

on *platinum* electrodes [1]. As indicated in [4] the

0021–891X/86 $03.00 + .12

electrode material strongly influences the anodic reaction products.

The reduction reactions of transition metal species are of interest as they pertain to the characteristics of battery cathodes incorporating those metals. Any material used for a practical battery with a room temperature nitrate–amide electrolyte must have a favourable reduction potential and a low cathodic overpotential at the maximum design current density to prevent the undesirable reduction of the melt and the evolution of gaseous products.

2. Experimental details

All chemicals used in this study were reagent grade or higher purity. Ammonium nitrate was dried under vacuum at 120–150° C for several days before use. Acetamide was dried under vacuum (pressure less than 1 Torr) over P_2O_5 for several days before use. Nickel (II) chloride and copper (II) chloride were used as received after drying under vacuum at 120–150° C. It should be noted that this procedure does not produce anhydrous metal halide salts; trace water held in the coordination sphere must be assumed present. All melts were prepared, stored and handled in an atmosphere of flowing air that had been dried to less than 0.5% relative humidity. Each melt was prepared by fusing the components with occasional agitation in a sealed Pyrex vessel at 120° C. Once the mixture was completely liquid, the melt was cooled to room temperature in an atmosphere of dry air. Karl Fischer analysis of melts prepared in this manner showed a normal water content less than 0.05 wt % H_2O. Metal ion solutions in the ammonium nitrate–amide melts were prepared by fusing the metal halide with the nitrate and the amides at 120° C in sealed Pyrex vessels.

All of the experiments reported here used a room temperature nitrate–amide ionic liquid consisting of an ammonium nitrate-supporting electrolyte (0.2 mol fraction) in an amide solvent composed of urea (0.4 mol fraction) and acetamide (0.6 mol fraction). The room temperature conductivity of this melt exceeded $10^{-3}\,\Omega^{-1}\,cm^{-1}$ [1]. We will use the term 'ammonium nitrate–amide melt' to refer to this composition in this communication.

Nickel corrosion experiments were performed by sealing a length of 22-gauge wire (99.9% pure) with the ammonium nitrate–amide melt at 120° C in a Pyrex vessel. Copper corrosion was studied using fine copper powder in the room temperature ammonium nitrate–amide melt. Corrosion products with similar spectra were formed by corroding copper wire in long-term (several months) experiments at room temperature.

Cyclic voltammetric experiments used a BAS cyclic voltammetry unit (Model CV-1B). This unit is not capable of compensating for *IR* drop. Hence, all results are reported uncorrected for *IR* effects. The electrochemical cell was the conventional three-electrode design using working electrodes sealed in either glass (platinum) or Teflon (silver). The counter electrode was a platinum foil and the reference electrode was a silver wire for the nickel studies and a copper wire for the copper studies. Measurements of these versus a saturated ferrocene/ferrocinium internal standard in the melt gave the potential of the copper wire of ~ 0.30 V versus Cp_2Fe/Cp_2Fe^+. The potential of the silver wire quasi-reference was ~ -0.10 V versus the Cp_2Fe/Cp_2Fe^+ couple. For further reference, the Cp_2Fe/Cp_2Fe^+ couple lies ~ 0.75 V positive of the lead wire quasi-reference used in earlier studies [1, 2]. We have found that the lead wire quasi-reference does not provide a stable reference potential in nitrate–amide melts containing either cupric chloride or nickel (II) chloride. All potentials are reported versus the reversible saturated ferrocene/ferrocinium redox potential on a platinum electrode [11]. Scans started at zero volts, proceeded cathodic, anodic, cathodic, then back to zero volts. Cyclic voltammetry experiments were conducted in an argon atmosphere using melts saturated with argon that had been dried over P_2O_5. Cyclic voltammograms were recorded on a Houston *x–y* recorder (Omnigraphic). Ancillary equipment used for this study included a Keithley (Model 225) constant current source, a PAR (Model 371) potentiostat/galvanostat and a Houston Instruments *y–t* recorder (Omniscribe). Ultraviolet–visible spectra of the metal ion solutions were recorded from 350 to 850 nm using a Beckman (Model DU-7) ultraviolet–visible spectrophotometer with quartz cells.

3. Results

3.1. *Reactions of nickel in NH_4NO_3–amide melts*

Fig. 1 shows the cyclic voltammetric responses of a platinum and a gold electrode in the ammonium nitrate–amide melt. Of particular interest are the oxidation and reduction limits of the melt and the large peak on the anodic sweep after melt reduction on platinum. This peak is quite similar to the oxidation of adsorbed hydrogen observed in aqueous acid solution [12]. Note that the cyclic voltammetry of the melt on a gold electrode has no corresponding wave. Since gold adsorbs hydrogen far less readily than platinum, the adsorbed hydrogen peak observed on the platinum electrode is absent on gold electrodes.

When nickel (II) chloride is fused with the ammonium nitrate–amide melt, the cyclic voltammetric responses observed in Fig. 1 are changed markedly. Fig. 2 shows the cyclic voltammetric responses of 0.01 mol fraction $NiCl_2$ in the ammonium nitrate–amide melt on a platinum wire electrode. The cyclic voltammogram was determined at 23° C in an argon-saturated melt. A reduction wave is noted near −0.14 V

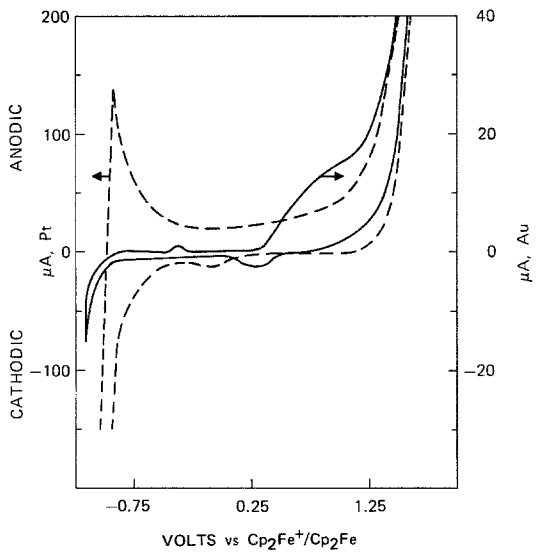

Fig. 1 Cyclic voltammetric studies of the ammonium nitrate–amide melt at 23° C on gold (area = 0.2062 cm^2) and platinum (area = 0.4791 cm^2) wire electrodes at 100 mV s^{-1}

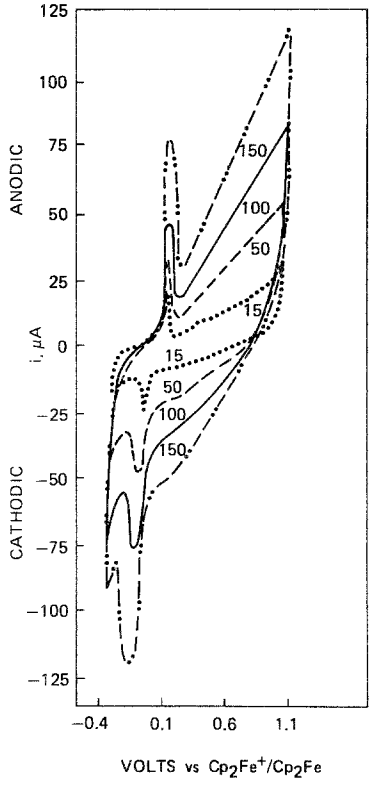

Fig. 2 Cyclic voltammetry studies of 0.02 mol fraction $NiCl_2$ in the ammonium nitrate–amide melt at 23° C as a function of scan rate. The working electrode was platinum (area = 0.229 cm^2).

(versus Cp_2Fe/Cp_2Fe^+). As the switching potential for the change from cathodic to anodic scans is moved more positive and out of the region of solvent reduction, two events occur. First, the height of the adsorbed hydrogen wave (peak C in Fig. 3) decreases; second, the height of the wave (peak E) that corresponds to the formation of platinum oxide from the oxidation of water on the platinum electrode decreases. These observations are reasonable since water can be formed during solvent reduction, the reduction of nitrate to nitrite and oxide species. Hydrogen is adsorbed on the electrode during solvent reduction. The height of both the second oxidation wave (peak D) and the corresponding reduction wave (peak A) is affected dramatically by a shift in the cathodic switching potential. When the working electrode is subjected to large cathodic currents (that involve appreciable nitrate reduction) the large quantities of ammonia gas, water and nitrite ions formed

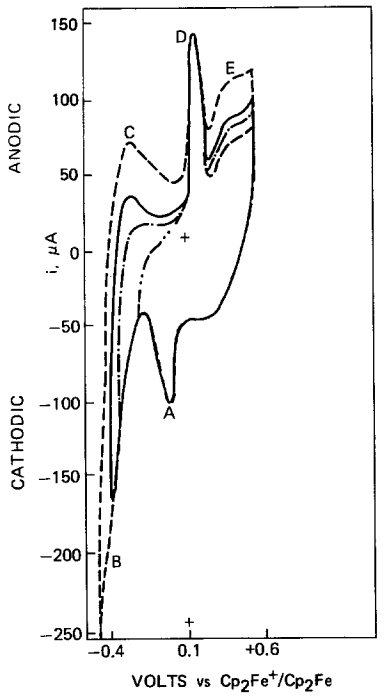

Fig. 3. Cyclic voltammetric responses of 0.02 mol fraction $NiCl_2$ in the ammonium nitrate–amide melt as the switching potential is moved cathodic. All of the scans were performed at 100 mV s^{-1} on a platinum electrode (area = 0.229 cm^2) in a 23° C, argon-saturated melt.

during the reduction change the shape of the oxidation waves. After sweeping well into the solvent reduction wave (peak B), a decrease in the peak heights of both the second oxidation wave (peak D) and the adsorbed hydrogen oxidation wave (peak C) is observed.

Current reversal chronopotentiometric experiments (in unstirred solutions) of the nickel ions (added as $NiCl_2$) in ammonium nitrate–amide melts provide further interesting information about the chemistry of nickel ions in nitrate–amide melts. Fig. 4 shows several representative analyses in 0.02 mol fraction $NiCl_2$ in the ammonium nitrate–amide melts. We find that there is only one distinct reduction process. A subsequent oxidation at the same (geometrical) current density shows one distinct oxidation process that occurs before solvent oxidation. Several ill-defined shoulders are observed on both oxidation and reduction processes over a wide range of current densities. We note that there is some gas evolution from the electrode during both the reduction and oxidation extremes. When a platinum cathode is set at 15–30 mA cm^{-2} for prolonged periods, a black deposit with a metallic luster and a large surface area is formed on the electrode surface. This deposit appears to corrode when left at open circuit. The corrosion products are deep blue. Nickel wire also corrodes in the ammonium nitrate–amide melts, producing a deep blue solution. For this reason, the long term stability of nickel-containing cathodes in ammonium nitrate–amide melts is open to question.

Fig. 5 shows the ultraviolet–visible near–infrared spectra of the $NiCl_2$ solution in the NH_4NO_3–amide melt (curve A). A background curve is shown for the nickel-free melt (curve B) and the spectra of a nitrate–amide melt after a nickel corrosion experiment conducted at 120° C for 2 h (curve C).

3.2. *The reactions of copper in ammonium nitrate–amide melts*

When copper (II) chloride is fused with the ammonium nitrate–amide melt, the cyclic voltammetric responses are quite different from those observed in either the pure melts (Fig. 1) or the $NiCl_2$ melts (Fig. 2). Fig. 6 shows the cyclic voltammetric responses of a 0.01 mol fraction $CuCl_2$ in the ammonium nitrate–amide melt on a platinum wire electrode. The cyclic voltammograms were determined at 23° C in an argon-saturated melt.

Copper metal corrodes in the ammonium nitrate–amide melts producing a blue–green complex. As a result, cathodes which reduce a copper species to copper metal may allow the formation of soluble cupric corrosion products that could, in turn, react with the anode. The ultraviolet–visible spectra of both the $CuCl_2$ solution and of the corrosion products are shown in Fig. 7 as curves A and B,. respectively. The copper corrosion products, like those of nickel, show absorption peaks shifted considerably blue of those of the metal chloride in solution.

Constant current reduction followed by constant current oxidations in unstirred ammonium nitrate–amide melts provide further information about the reactions we are investigating. Fig. 8 shows several representative plating

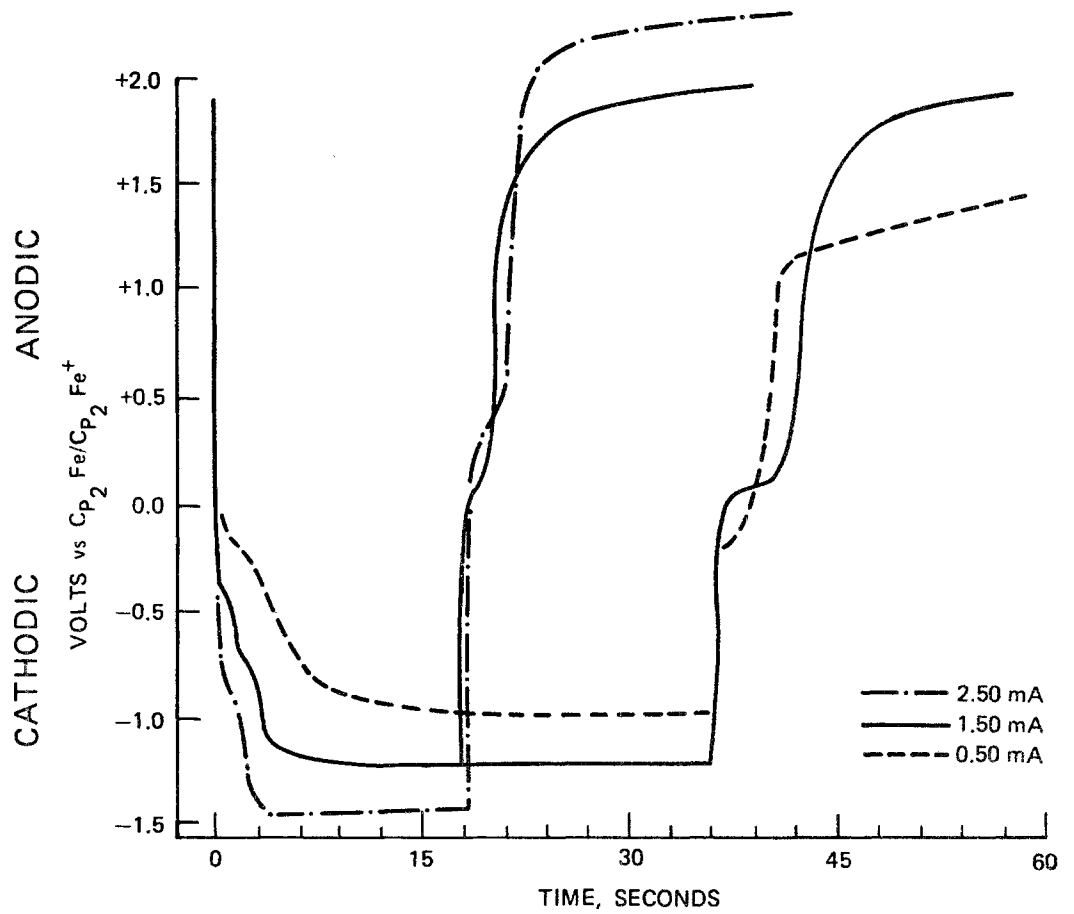

Fig. 4. Typical chronopotentiometric responses of an 0.02 mol fraction $NiCl_2$ in the ammonium nitrate–amide melt. The working electrode was a platinum wire (area = 0.229 cm^2) in a 23° C, quiescent melt.

and stripping experiments in the ammonium nitrate–amide melts. We note that there is some gas evolution from the electrode during the reduction. When the cathode is set at 1–5 mA cm^{-2} for prolonged periods, a spongy copper-coloured deposit with a metallic luster is formed. During the long-term electrolysis the melts gradually becomes colourless.

4. Discussion

4.1. *Reactions of nickel in nitrate–amide melts*

Nickel ions in the $NiCl_2$–ammonium nitrate–amide melt can be reduced in a two-electron step to nickel metal during high current density reductions:

$$Ni^{2+} + 2e \longrightarrow Ni^0 \qquad (3)$$

This is evidenced primarily by the visible production of nickel metal deposits during long-term electrolysis. The nickel deposited during chronopotentiometric reductions is readily oxidized both by corrosion reactions and by the chronopotentiometric oxidation of the deposited metal. The reduction of nickel ions must occur at a potential close to the solvent reduction wave. Nickel ion reduction is present in the cyclic voltammograms only as a poorly defined shoulder on the solvent reduction wave at very high current density. It seems improbable that the simple reduction of nickel ions could be responsible for the waves observed as positive as 0.1 V.

The electrodeposition of nickel has been

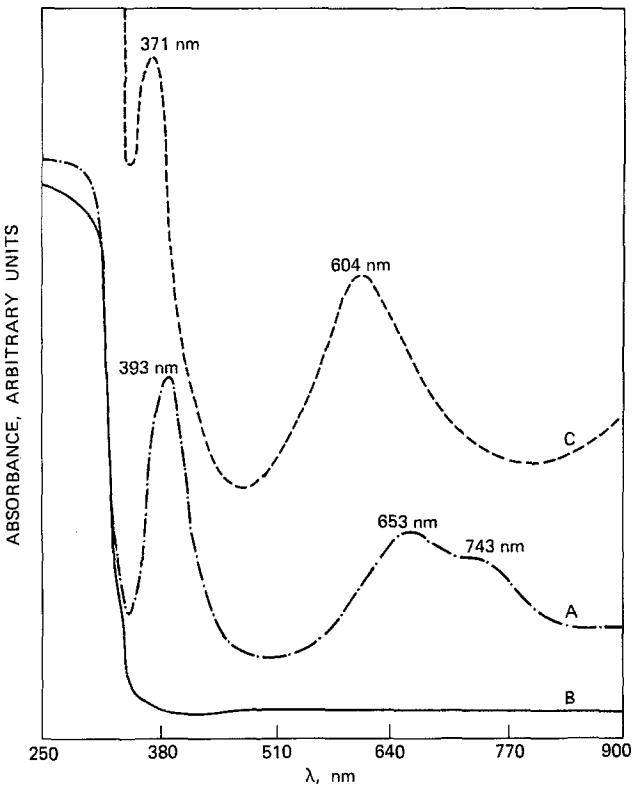

Fig. 5. Ultraviolet–visible spectra of the blank melt in a 1 cm cell (curve B), the 0.02 mol fraction $NiCl_2$ in the ammonium nitrate–amide melt in a 0.01 cm cell (curve A) and the nickel corrosion products in a 0.5 cm cell (curve C). The *y*-axis is in arbitrary absorbance units.

demonstrated by several investigators using several primary alkyl amides including formamide [13–15], acetamide [13] and urea [16]. The electrodepositions are reported to be irreversible [17]. Lovering *et al.* reported that the addition of traces of water to an anhydrous $LiNO_3$–KNO_3 melt at 145° C changed the essentially reversible reduction of nickel ions into an irreversible reaction [18]. Since amides, like water, often coordinate through the oxygen atom [19], we can draw certain analogies between aquo and primary amide coordination. We attribute the observed irreversibility of the nickel electroreduction in nitrate–amide melts to the tenacity of the nickel–amide carbonyl oxygen bonds that are similar to the aqueous solution effects attributed to the 'tenacity of the aquo–nickel bonds' [20].

The cyclic voltammetric studies shown in Figs 2 and 3 have shown that there is one clearly related redox couple present in the nickel (II) chloride–ammonium nitrate–amide melt. These reactions occur near +0.1 V versus the reversible ferrocene/ferrocinium couple. Both waves are extremely sensitive to the condition and history of the electrode surface and the melt. Cyclic voltammetric scans that proceed to extremely negative potentials tend to broaden the peak current of the reduction wave. The oxidation wave retains a relatively sharp waveform even after these high rate reductions.

A similar sharp 'redox' pair is observed when zinc chloride is added to the nitrate–amide melt. These 'sharp waves' have thus far defied adequate explanation and are the subject of an ongoing investigation in this laboratory. It seems quite likely that the origin of the 'sharp waves' is a reaction involving a nickel (or zinc) complex ion; this might involve the presence of aquo ligands in the coordination sphere.

The main corrosion reaction of nickel in the ammonium nitrate–amide melt appears to be

$$Ni + 2NH_4NO_3 \longrightarrow Ni^{2+} + 2NH_3 + 2NO_3^- + H_2 \qquad (4)$$

The nickel ions formed by the corrosion reaction could then form a nickel–amide–ammonia complex. The effect of the stronger bonding

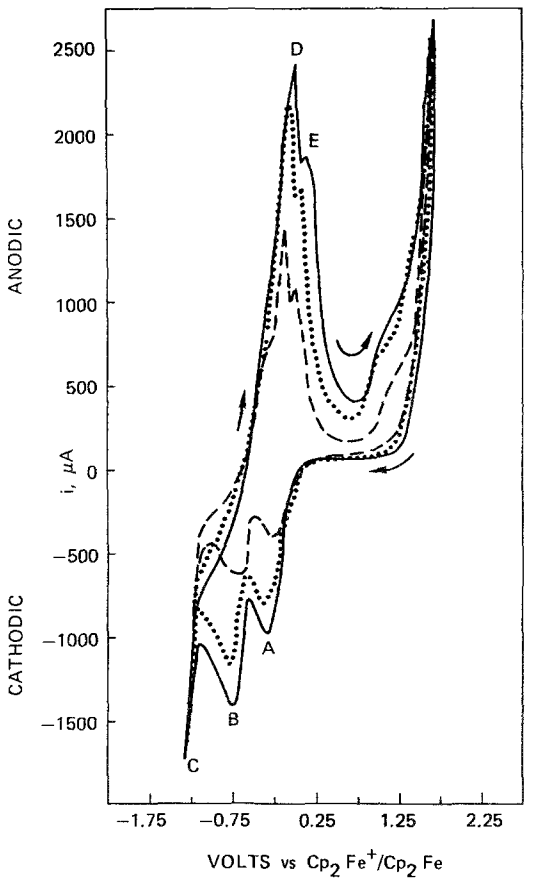

Fig. 6. Cyclic voltammetry studies of 0.01 mol fraction $CuCl_2$ in the ammonium nitrate–amide melt at 23° C as a function of scan rate. The working electrode was platinum (area = 0.229 cm^2).

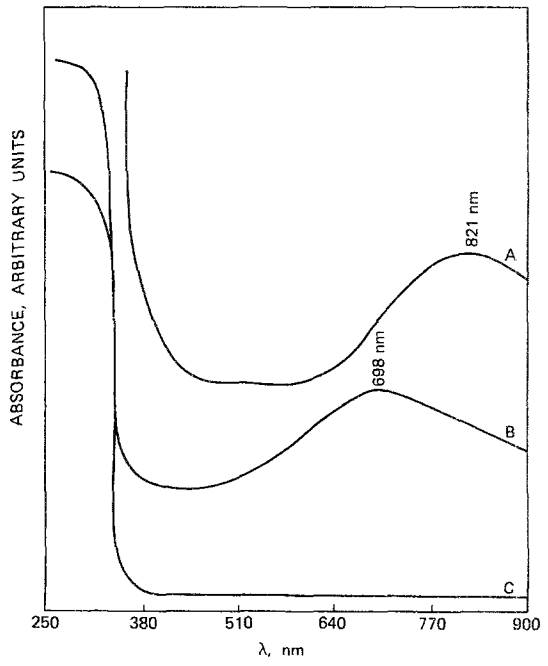

Fig. 7. Ultraviolet–visible spectra of the blank melt in a 1 cm cell (curve C), the 0.02 mol fraction $CuCl_2$ in the ammonium nitrate–amide melt in a 0.01 cm cell (curve A) and the copper corrosion products in a 0.01 cm cell (curve B). The y-axis is in arbitrary absorbance units.

ammonia ligands would have two spectroscopic manifestations. First, the spectra of the ammonia-coordinated complex shows no $^3T_{1g}$ (F) to ^1E splitting that is associated with d8 complexes with a weak ligand field. Second, the strongly binding NH_3 group blue shifts the absorption maxima. The spectrum of the corrosion products agrees quite well with published interpretations of $[Ni(NH_3)_6]^{2+}$ in an octahedral ligand environment [21]. Simply bubbling NH_3 gas into a solution of $NiCl_2$ in the NH_4NO_3–amide melt produces a similar, deep blue complex.

The following assignments may be made to the spectra of the ammonia-coordinated corrosion products shown in Fig. 5: the $^3A_{2g}$ to $^3T_{1g}$(P) transition produces an absorption band at 371 nm (26 594 cm^{-1}), and the $^3A_{2g}$ to $^3T_{1g}$ (F) transition produces a band at 604 nm (16 556 cm^{-1}). No $^3T_{1g}$ (F) to ^1E splitting is observed in the corrosion products.

The ultraviolet–visible spectra of the nickel ions in solution show three distinct peaks at 393 nm (25 445 cm^{-1}), 653 nm (15 314 cm^{-1}) and 743 nm (13 459 cm^{-1}). Given that the ground state configuration of the d8 nickel ions in an octahedral environment is $^3A_{2g}$, the peak at 393 nm corresponds to the $^3A_{2g}$ to $^3T_{1g}$ (P) transition. The close bands at 653 and 743 nm suggest that the ligand field environment is weak and that there is significant splitting between the ^1E and $^3T_{1g}$ (F) states. The band at 653 nm may be assigned to the $^3A_{2g}$ to ^1E transition, while the transition to the $^3T_{1g}$ (F) state is responsible for the band at 743 nm [22–25]. Other researchers have reported that $[Ni(acetamide)_6]^{2+}$ complexes in acetone [23] and in molten acetamide [24] show three transitions in the visible at wavelengths near to those we observe in the ammonium nitrate–amide melt. Studies of $[Ni(urea)_6](ClO_4)_2$ complexes have shown that

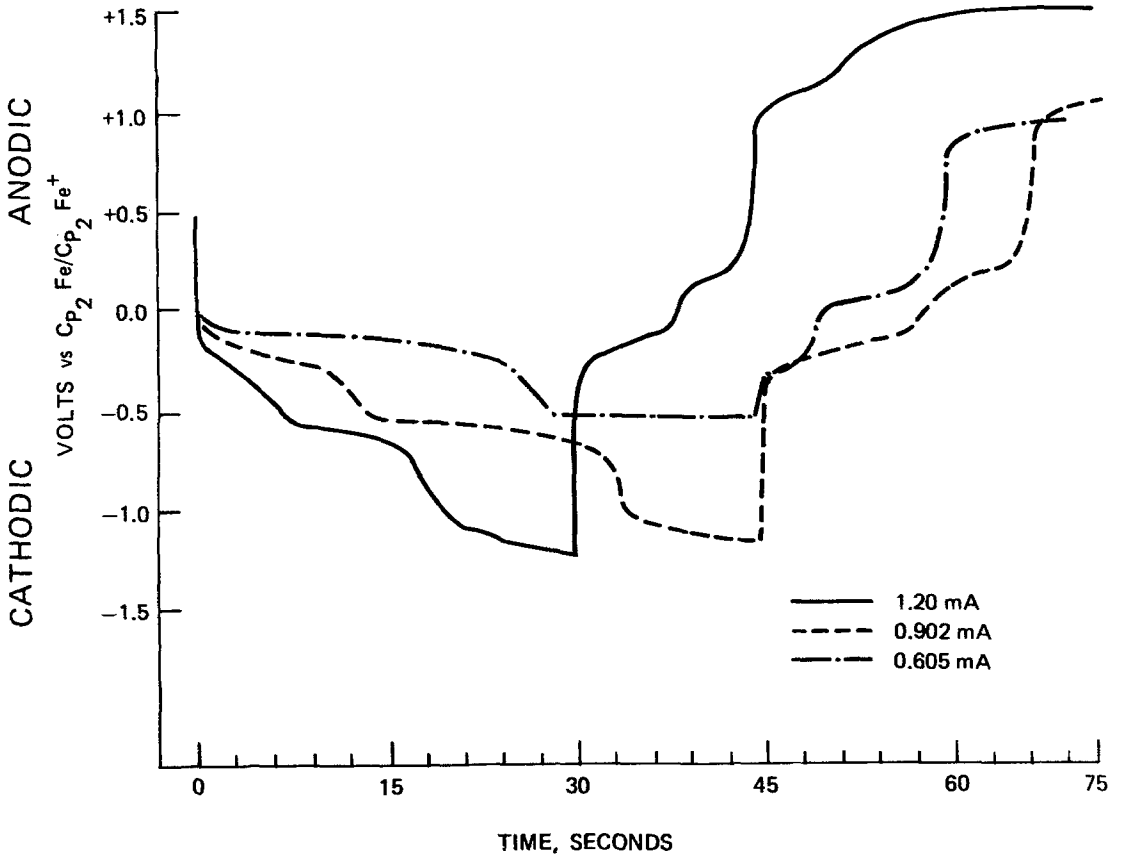

Fig. 8. Typical chronopotentiometric responses of a 0.02 mol fraction $CuCl_2$ in the ammonium nitrate–amide melt. The working electrode was a platinum wire (area = 0.299 cm^2) in a 23° C, quiescent melt.

the urea ligand bonds less strongly than acetamide [25].

Given the close agreement between the reported values for the transitions of the $[Ni(acetamide)_6]^{2+}$ complex and the values we determine in the ammonium nitrate–amide melt, it seems quite likely that the $NiCl_2$ added to the melt forms a $[Ni(amide)]^{2+}$ complex with at least two amide ligands. The nickel corrosion reaction almost certainly produces a complex coordinated by one or more ammonia ligands.

4.2. *Reactions of copper in nitrate–amide melts*

The two distinct reduction processes (waves A and B in Fig. 6) probably correspond to the simple two-step reduction of copper

$$Cu^{2+} + e \longrightarrow Cu^{+} \quad (5)$$

$$Cu^{+} + e \longrightarrow Cu \quad (6)$$

All of the peaks in the cyclic voltammograms of $CuCl_2$ on platinum show linear relationships between the peak currents and the square root of the scan rates over the range of scan rates (15–150 mV s^{-1}) studied. The oxidative sweep shows two distinct waves (labelled D and E in Fig. 6) that appear to correspond to the oxidation of copper metal to cuprous and then to cupric ions:

$$Cu \longrightarrow Cu^{+} + e \quad (6a)$$

$$Cu^{+} \longrightarrow Cu^{2+} + e \quad (6b)$$

At the faster scan rates, the second (more anodic) process becomes less distinct and may be lost in the intense copper metal oxidation wave.

We note that an electrochemical study of cupric and cuprous ions in *N,N*-dialkyl amides presents evidence for the reduction of Cu^{2+} to Cu^{+} followed by the reduction of Cu^{+} to copper

metal [26]. The presence of two distinct waves in the oxidation and reduction processes during current reversal chronopotentiometry suggests that the cuprous ion may also be stable in these melts.

The observed blue discolouration of the melts by the corrosion reaction may be readily explained by a reaction similar to that which we observe on nickel

$$Cu + 2NH_4NO_3 \longrightarrow$$
$$Cu^{2+} + 2NH_3 + 2NO_3^- + H_2 \qquad (7)$$

Free ammonia ligands produced by the corrosion reaction could coordinate copper ions (presumably cupric) at the corrosion site. Unfortunately, we can find no references to the ultraviolet–visible spectrum of copper complexes with simple primary alkyl amides in the absence of water. As a result, we cannot compare the spectra of our $CuCl_2$ solution and our corrosion product spectra with any published results. However, given the differences in the two spectra, we can safely conclude that the $CuCl_2$ solution in the ammonium nitrate–amide melt forms a copper–amide complex that is a distinctly diffferent species from the complex formed by the corrosion reaction. We note that both the corrosion products and the cupric chloride solution show a single significant absorption peak in the visible, suggestive of a d9 (Cu^{2+}) cation rather than the lack of absorptions in the visible that would indicate a d10 (Cu^+) species [27]. Also, since the spectra of the corrosion product has an absorption maxima significantly blue of those of the simple ions in solution, we can conclude that the complex formed by the corrosion reaction is bound by at least one ligand that is higher in the spectrochemical series than the amides that coordinate cupric ions in the simple cupric chloride solution. This leads us to the conclusion that the corrosion product complex is coordinated by at least one ammonia ligand. Cupric ions are known to act as weak acids in molten amides [28, 29]. These copper–amide complexes form $Cu(R–CONH)_2$ species in solution. It seems likely that the other coordination sites are occupied by undissociated amides.

In the analysis of the spectrum of the copper corrosion products, we note that the visible spectra of the copper corrosion products has a single major peak at 698 nm. The interpretation of individual spectral transitions for the corrosion products in solution is complicated by the extremely high spin-orbit coupling constant of copper [30]. A detailed characterization of the symmetry of the copper complexes in solution is beyond the scope of this work. However, given the higher energy of the absorption bands of the corrosion products, it seems likely that the corrosion product has one or more of the sites in the first coordination sphere (that are occupied by amides in the simple copper chloride solutions) occupied by one or more ammonia ligands.

5. Conclusions

Both nickel and copper display an interesting electrochemistry and spectrochemistry in nitrate–amide melts. Both metals corrode in the nitrate–amide melts, and both corrosion reactions produce products that show spectra that lie considerably blue of the simple solutions of the ions in the melt free of corrosion products. This has been attributed to the formation of a metal–amide–ammonia complex. Simple solutions of the metal halides in the ammonium nitrate–amide melts are primarily amide coordinated.

The reduction of Cu(II) ions proceeds via the Cu(I) ion to the metal. Both of these reactions are reversible and the corresponding oxidation reactions are observed.

Cyclic voltammetric responses in Ni^{2+} solutions are quite dependent on the history of the electrode. Two anodic processes may be observed: the first of these is the oxidation of adsorbed hydrogen on the electrode surface; the second process is of unknown origin. Nickel ions may be reduced to nickel metal. However, this process occurs close to the melt reduction potential. One characteristic feature of the cyclic voltammograms of the $NiCl_2$ solution is the presence of a sharp, well defined 'redox' couple. A similar couple is observed in $ZnCl_2$ solutions and may relate to a complex species either in solution or adsorbed in the electrode.

Both nickel and copper salts may prove useful cathode material for short-term ambient temperature battery systems using nitrate–amide

ionic liquid electrolytes. However, the corrosion of deposited nickel and copper metal raises questions about the long-term stability of cathodes using these materials.

Acknowledgements

The authors wish to acknowledge support of this work by the Office of Naval Research. We also wish to acknowledge valuable comments by Dr David G. Lovering (Royal Military College of Science, Schrivenham, Swindon, Wilts., UK).

References

[1] G. E. McManis, A. N. Fletcher, D. E. Bliss and M. H. Miles, *J. Electroanal. Chem.* **190** (1985) 171.
[2] *Idem, J. Appl. Electrochem.* **16** (1986) 101.
[3] D. G. Lovering and R. J. Gale (eds), 'Molten Salt Techniques', Vol. 1, Plenum Press, New York (1983) p. 5.
[4] D. G. Lovering and K. P. D. Clark, 'Proceedings 4th International Molten Salts Symposium', (edited by M. Blander), The Electrochemical Society, Inc., Pennington, NJ (1984) p. 603.
[5] D. A. Tkalenko, S. A. Kudrya and A. A. Rudnitskaya, *Elektrokhimiya* **14** (1978) 140.
[6] A. A. Rudnitskaya, S. A. Kudrya and D. A. Tkalenko, *Ukrain. khim. Zhur.* **44** (1978) 367.
[7] L. I. Antropov, D. A. Tkalenko and S. A. Kudrya, *Elektrokhimiya* **11** (1978) 1832.
[8] D. S. Cherepanov, S. Chernukhin and N. Kh. Tumanova, *Ukrain. khim. Zhur.* **47** (1981) 563.
[9] I. M. Bokhovkin, Yu. I. Bokhovkina and E. O. Vitman, *Zhur. Obshchei. Khim.* **34** (1964) 2826.
[10] L. S. Bleshchinskaya, K. Sulaimankulov and M. D. Davranov, *Russ. J. Inorg. Chem.* **28** (1983) 607.
[11] A. J. Bard and L. R. Faulkner, 'Electrochemical Methods', John Wiley, New York (1980) p. 701.
[12] P. Delahay, 'Double Layer and Electrode Kinetics', John Wiley, New York (1965) p. 242.
[13] L. F. Ytnema and L. F. Audrieth, *J. Amer. Chem. Soc.* **52** (1930) 2693.
[14] S. Sultan and P. K. Tikoo, *Surf. Technol.* **21** (1984) 233.
[15] L. F. Audrieth, L. F. Yntema and H. W. Nelson, *Trans. III. Acad. Sci.* **23** (1931) 302.
[16] K. K. Bansal and M. L. Anand, *J. Ind. Chem. Soc.* **50** (1983) 33.
[17] V. Bartocci, M. Guster, R. Marass, F. Pucciarelli and R. Cescon, *J. Electroanal. Chem.* **94** (1978) 153.
[18] D. G. Lovering and R. M. Oblath, *J. Electrochem. Soc.* **127** (1980) 1997.
[19] M. S. Barvinok and L. V. Mashkov, *Zh. Neorg. Khim.* **25** (1980) 445.
[20] D. G. Lovering, *Coll. Czech. Chem. Commun.* **37** (1972) 3697.
[21] A. G. Sharpe, 'Inorganic Chemistry', Longman, London, (1981).
[22] A. B. P. Lever, 'Inorganic Electronic Spectroscopy', Elsevier, Amsterdam (1968) p. 333.
[23] R. S. Drago, D. W. Meek, M. D. Joesten and L. LaRoche, *Inorg. Chem.* **2** (1963) 124.
[24] M. E. Stone and K. E. Johnson, *Can. J. Chem.* **49** (1971) 3836.
[25] P. W. N. M. Van Leeuwen and W. L. Groenveld, *Rec. Trav. chim.* **87** (1968) 86.
[26] K. W. Bayer and R. T. Iwamoto, *J. Electroanal. Chem.* 7 (1964) 458.
[27] F. A. Cotton and G. Wilkinson, 'Advanced Inorganic Chemistry', 4th edn, John Wiley, New York (1980) p. 800.
[28] M. Pournaghi, J. Devynck and B. Tremillion, *Analyt. Chim. Acta* **89** (1977) 321.
[29] G. Jander and G. Winkler, *J. Inorg. Nucl. Chem.* **9** (1959) 24.
[30] S. Sultan and P. K. Tikoo, *Surf. Technol.* **21** (1984) 355.